e official journal of the International Association for Mathematical Geology
nding Editor: Daniel F. Merriam

nt-outside cover: Student exercise in subsurface structure, contour mapping, and rudimentary petroleum logy. From a contour map of a hypothetical structure and placement of dry holes, students are asked to site wells in the most promising grid cells with no current production. Figure provided by Ronald R. McDowell.

hematical Geology (ISSN: 0882-8121), the official journal of the International Association for Mathematical Geology, is published monthly except March, June, September, and December for the International Association for Mathematical Geology by Kluwer demic/Plenum Publishers, P.O. Box 322, 3300 AH Dordrecht, The Netherlands. Annual subscription price U.S. $819.00. Air freight mailing by Publications Expediting, Inc., 200 Meacham Avenue, Elmont, N.Y. 11003. *Mathematical Geology* is abstracted or indexed quatic Science and Fisheries Abstracts, Chemical Abstracts, COMPUMATH Citation Index, Computer and Information Systems tracting Journal, Current Contents/Physical, Chemical and Earth Sciences, Geotitles, Mathematical Reviews database, Petroleum tracts, Referativnyi Zhurnal, Science Citation Index, Science Citation Index Expanded, The ISI Alerting Services, and Water Resources Abstracts, Zentralblatt fur Mathematik. 0882-8121/03

vertising inquiries should be addressed to the Advertising/Sales Manager, Kluwer Academic Publishers, 101 Philip Drive, Assinippi rk, Norwell, Massachusetts 02061, USA—telephone (781) 871-6600 and fax (781) 871-6528.

bscription inquiries and subscription orders should be addressed to the publisher as follows: For all countries (including subscription ents in North and Latin America): Kluwer Academic Publishers, Journals Department—Distribution Centre, PO Box 322, 3300 AH rdrecht, The Netherlands; tel: 31 78 657 6000; fax: 31 78 657 6474; e-mail: orderdept@wkap.nl. For "non-trade" customers only in rth, South, and Central America: Kluwer Academic Publishers, Journals Department, 101 Philip Drive, Assinippi Park, Norwell, MA 061, USA; tel: 1 781 871 6600; fax: 1 781 681 9045; e-mail: kluwer@wkap.com. Subscription rates:
Volume 35, 2003 (8 issues): Print or electronic, EUR 891.00/USD 819.00/GBP 573.00.
Volume 36, 2004 (8 issues): Print **or** electronic, EUR 958.00/USD 880.00/GBP 630.00. Print *and* electronic, EUR 1149.60/USD 1056.00. For more information about our 2004 journal prices, visit www.kluweronline.com.

Stochastic Structural Modeling[1]

Lars Holden,[2] Petter Mostad,[2] Bjørn Fredrik Nielsen,[2] Jon Gjerde,[2] Chris Townsend,[3] and Signe Ottesen[4]

A consistent stochastic model for faults and horizons is described. The faults are represented as a parametric invertible deformation operator. The faults may truncate each other. The horizons are modeled as correlated Gaussian fields and are represented in a grid. Petrophysical variables may be modeled in a reservoir before faulting in order to describe the juxtaposition effect of the faulting. It is possible to condition the realization on petrophysics, horizons, and fault plane observations in wells in addition to seismic data. The transmissibility in the fault plane may also be included in the model. Four different methods to integrate the fault and horizon models in a common model is described. The method is illustrated on an example from a real petroleum field with 18 interpreted faults that are handled stochastically.

KEY WORDS: reservoir characterization, faults, horizons, unfaulting, structural reconstruction, reservoir uncertainity.

INTRODUCTION

The structural model of a reservoir is a common model for geological horizons and faults. It forms the geometrical framework for the 3D grid, providing the boundaries for the facies and petrophysical models which describe the rock properties. Furthermore it forms the basis for volumetric calculations, well planning, and reservoir simulation grids.

Both seismic and well data provide important information regarding the structural model, but even so there is still considerable uncertainty. This paper describes a stochastic model for the reservoir structure that may be used to represent this uncertainty. The model may be conditioned on seismic and well data, while still allowing efficient simulation of realizations. These realizations can be used as input to facies and petrophysical modeling, and in the generation of the reservoir simulation grid. The uncertainty in the structural model is neglected in most reservoir

[1]Received 26 April 2002; accepted 10 June 2003.
[2]Norwegian Computing Center, Blindern, Oslo, Norway; e-mail: jon.gjerde@nr.no
[3]Nederlandse Aardolie Maatschappij B.V., Assen, The Netherlands.
[4]Statoil, Stavanger, Norway.

studies. The reason is that changes in the structural model imply changes in the facies and petrophysical models and in the reservoir simulation grid. Traditionally, there is a considerable amount of work involved for each change of the structural model. However, the structural model uncertainty is usually very important both for volume estimates and for flow properties. This is a large-scale effect that cannot be averaged out. The only realistic way to handle the uncertainty in 3D models is to generate several realizations. The key is to generate these in such a way that building facies, petrophysical, and simulation models are done automatically for each realization. Thore and others (2002) describe ways of defining the structural uncertainty and also suggest a different workflow for modeling it. The main difference from the workflows presented in this paper is that Thore and others (2002) lack the possibility of unfaulting and refaulting the horizons and grids, and does not also include the possibility of calculating fault fluid flow properties for the different realizations within their workflow.

The stochastic model presented here builds on the Horizon model presented in Abrahamsen (1992), in which the horizons are modeled as Gaussian fields. The fault model is part of the Havana model presented in Hollund and others (2000). This includes a description of the displacement operator, whereby finite displacement occurs along fault surfaces and infinitesimal displacements occur in the volume surrounding the fault. This facilitates the modeling of geological features that were continuous before faulting, like horizons or facies bodies, and is thus most important for representing post-sedimentary faults. It is also helpful for performing structural reservoir reconstruction both for post-sedimentary and syn-sedimentary faults.

In this paper it is focussed on the seismic observable faults. In some studies this is combined with the subseismic faults as described in Hollund and others (2003). In this fully integrated model, the horizons and fault surfaces are given flow properties depending on the rock properties close to these surfaces. We will assume that the reservoir simulation grid has linear pillars as is usual in commercial software packages.

THE STRUCTURAL MODEL

A stochastic structural model has been developed comprising two basic, but fully integrated, parts; a model for fault surfaces and their displacement operator and a model for the horizons.

The Fault Model

The fault model has been designed so that it represents the most important geometrical aspects of fault patterns. Fault displacement is also included in the

model and this allows for displacements to be both removed (i.e., unfaulting) and added to the geological horizons. The model uses a parametric representation that allows uncertainty in both fault geometry and displacement operator to be easily accounted for.

In the present model, a single fault is described by a number of linear pillars where each pillar is described by a single point (a center point), a vector describing the orientation of the pillar and a piecewise linear displacement operator. The number of faults, the number of pillars representing a fault, the truncation pattern, and time sequences of the faults are not changed in the stochastic model. However, it is possible to extend the model to include these properties stochastically.

The linear pillars that define a fault are connected with bilinear surfaces, see Figure 1. Additional pillars are also defined outside the fault surface, which control the displacement field away from the fault surface. The displacement operator is triangulated between the various pillars. This triangulation must be well defined for all points within the area of influence of the displacement operator.

For a single pillar a piecewise linear invertible function with finite support describes the displacement of points along it. The triangulation and the bilinear surfaces defined by the pillars divide the reservoir into regions. A point P in a triangle box (a triangular base in each horizontal plane) has local coordinates ω_1, ω_2 defined by the equation

$$P = P_3 + w_1(P_1 - P_3) + w_2(P_2 - P_3)$$

where P, P_1, P_2, P_3 are points in the same horizontal plane where the three last points are on the three pillars defining the triangle box. The displacement operator $f(z)$ is defined by

$$f(z) = (1 - \rho(w_1, w_2))^2(w_1 f_1(z) + w_2 f_2(z) + (1 - w_1 - w_2) f_3(z))$$

within the triangle box where $f_i(z)$ is the displacement operator on the three pillars in the corner of the triangle box and ρ is a linear function in the triangle equal to

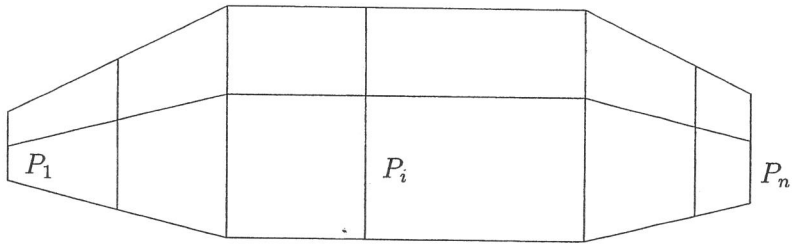

Figure 1. The figure illustrates the pillars denoting break lines and the bilinear surfaces in the fault plane.

0 at the fault plane and usually equal to 1 at the border of the influence area of the fault. The points are moved in the direction $w_1 v_1 + w_2 v_2 + (1 - w_1 - w_2) v_3$ where v_i is a vector in the direction of pillar P_i with vertical component 1. The pillars are assumed to have a large vertical component. The displacement is along the pillars. Hence, the displacement in strike-slip faults may not be modeled and an oblique-slip fault will be poorly modeled without a considerable extension of the model.

Displacements are calculated by applying each fault in a given sequence. The order of the faults in time must be specified since the total displacement depends on the fault order. X faults, i.e. that one fault disconnects the fault plane of another fault, is modeled by first applying the first fault and then the second fault without considering the first fault. If the order of the faults that are crossing each other are changed, then this changes the fault that is disconnected. Except for faults that truncate each other, all faults including the pillars are modeled independent of each other.

Fault truncations, branching, i.e. that one fault is only active on one side of the other fault, are allowed within the model. If Fault B is truncated by Fault A, Fault B will be split into two parts, a retained and a discarded part. Only the retained part of Fault B is active. It is required that Fault B does not move any point through Fault A and that the two faults planes intersect along a common line, called a branch line. The branch line may be a pillar in the two faults, but this is not required. Branch lines are often important in the process of gridding the reservoir. Branching faults are a y-fault in the xy plane. Figure 2 shows realizations of several branching faults. It is also possible to have a y fault in a xz or yz plane. Then the two faults should not have a common pillar and the displacement operator of Fault B must decrease to zero at the fault surface of the other fault. Such faults are difficult to represent using a corner point grid format defined by linear pillars. It can only be

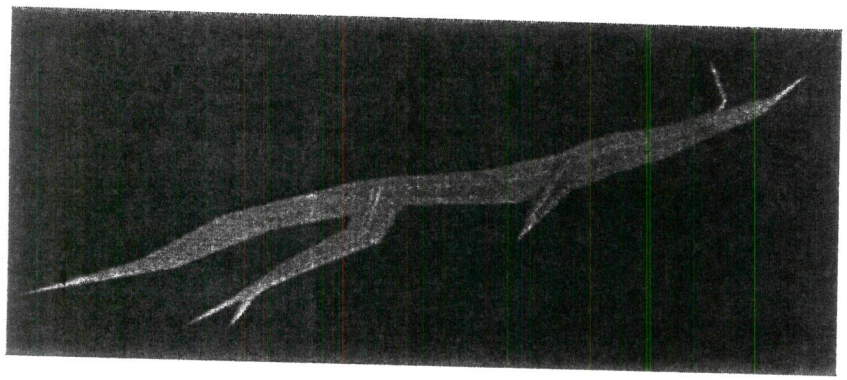

Figure 2. The figure illustrates the fault plan in a branching fault. This is represented as several faults that are truncated by the main fault.

represented by steps in the grid, where the resulting displacement is controlled by the layer thickness rather than the fault operator.

An important part of the fault model is the description of the fault surface properties. This is most efficiently represented as transmissibility multipliers and nonneighbor connections in the reservoir simulation grid. There are a number of papers on modeling fault seal depending on the shale or clay content on the layers on both sides of the faults, see Lindsay and others (1993), Yielding, Freeman, and Needham (1997), and Manzocchi and others (1999). Transmissibilities may also be calculated by simulating smaller faults in a fault zone, see Omre and Sølna (1990) and Omre and others (1992). Fault transmissibilities are in most cases very uncertain and may be one of the major uncertainties in a reservoir model, as concluded by Lia and others (1997). Hence, stochastic modeling of the transmissibilities is usually required. The model has several different methods for describing the transmissibilities of the fault surface depending on the shale and clay content of the facies on either side of the fault, and by modeling both the fault zone thickness and permeability as stochastic variables. The transmissibility multiplier calculations are also based on the dimensions of the surrounding reservoir simulation blocks.

The Horizon Model

It is convenient to describe the horizons as Gaussian fields, since Gaussian fields have a solid theory, see for example Journel and Huijbregts (1978). By including trends and using a variety of correlation functions, such fields should be sufficiently flexible to represent the horizons. In Abrahamsen (1992), an efficient stochastic model, named Horizon, is described. It has been used to model the horizons in a large number of field studies using seismic data and many deviated wells.

The horizons $H = (Z_0, \ldots, Z_n)$ satisfying $0 = Z_0(x, y) < Z_1(x, y) \leq Z_2(x, y) \leq \cdots \leq Z_{m+1}(x, y)$ are modeled by the equations

$$Z_{i+1}(x, y) = Z_i(x, y) + R_i(x, y) + \varepsilon_{i+1}(x, y) - \varepsilon_i(x, y) \quad \text{for } i = 1, \ldots, m$$

where

$$R_i(x, y) = \sum_j a_{i,j} g_{i,j}(x, y). \tag{1}$$

The stochastic fields Z_i and ε_i are Gaussian except for the truncations defined by the equations above. The user should specify prior distributions for $a_{i,j}$, the trend surfaces $g_{i,j}(x, y)$ that may be seismic reflection times, and the correlations in the noise fields $\varepsilon_i(x, y)$ that have zero expectation. In the equations above, horizon Z_{i+1} depends on Z_i for $i = 1, \cdots, m$. For some reservoirs it is better to model the

horizons in a different order because of less uncertainty in some horizons than in others. It is even possible to have more equations than horizons in order to constrain the model better.

Integrating Horizon and Fault Model

This paper describes four different approaches for integrating the fault and horizon models. Figure 3 illustrates the different approaches. In the first three

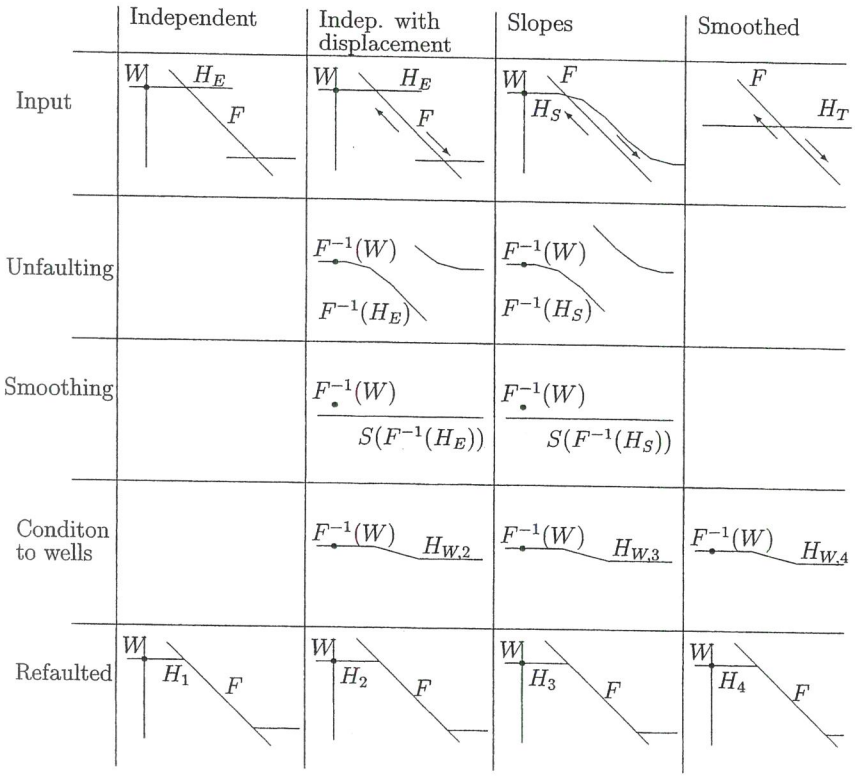

Figure 3. Four alternative methods for integrating horizons and faults in a consistent model. The horizons are denoted H_E when extrapolated, H_S when smoothed, H_T as a trend surface, and H_W when it is conditioned on unfaulted well data. W denotes a well and F denotes a fault. Independent: The fault truncates the extrapolated horizon. The fault displacement operator is not needed. Independent with displacement: The extrapolated horizon is unfaulted, smoothed, adjusted to fit unfaulted well data, and faulted. Slopes: The fault is modeled as a slope in the horizon model. The horizon is unfaulted, smoothed, adjusted to fit unfaulted well data, and faulted. Smoothed: The horizon is modeled as a smooth surface and conditioned on the unfaulted well data and afterwards faulted.

models the horizons are modeled as they are interpreted from seismic data, whereas in the fourth alternative, smoothed horizons are modeled. After the first three models are described, a separate section discusses some common properties of these three alternatives.

Independent Modeling

The fault surfaces and the horizons are modeled independently using this method. The horizons H_E are an extrapolation of the horizons $H = (Z_0, \ldots, Z_n)$ described above. After the faults and horizons are simulated, the fault surfaces truncate the horizons on either side of the fault described by the equation

$$H_1 = T_F(H_E)$$

where T_F is a truncation operator. The intersection lines are denoted hanging-wall and foot-wall cutoff lines. As horizons are usually poorly described close to faults, it is often necessary to use horizon information away from the fault and extrapolate this towards the fault surface. This method is used in several commercial 3D modeling software packages.

This approach has the disadvantage that information from one side of the fault cannot be used on the other side, both in the modeling of the horizons and reservoir properties. If trend data is used for example from seismic data, these will often not be defined close to the faults. All trend data must be extrapolated sufficiently far that the trend surface is always defined for all positions of the faults. Extrapolation may be a time-consuming manual job. One may give an increasing uncertainty at the extrapolated part of the surfaces.

Errors in input data are particularly critical in this alternative, since displacement operator is not used in a quality control and to correct errors. The extrapolation of horizons close to faults can produce erroneous results and are often difficult to correct. These errors are more pronounced where fault displacements are smallest or where horizons are highly irregular because of either folding or poor quality seismic data. The errors can include spurious displacements leading to incorrect stratigraphic juxtaposition across a fault and in some cases normal faults become reverse. If the displacement operator is to be estimated by the difference between the hanging-wall and foot-wall cutoff lines then inconsistencies will be introduced if this method is used. A structural reconstruction is not possible in this alternative since the displacement operator is not defined.

Independent Modeling With Displacement

In this alternative the fault displacement operator is also modeled. This makes it possible to unfault all the modeled horizons. Unfaulting an horizon using a

displacement operator to precisely remove the offset is very difficult. Therefore a smoothing operator is used after the displacement is approximately removed. This smoothing operator is denoted

$$S(F^{-1}(H_{\mathrm{E}}))$$

where H_{E} denotes the set of extrapolated horizons, F^{-1} the inverse of all the faults, and S the smoothing of all the horizons. Note that F^{-1} consist of one operation per fault applied in a specified time sequence. We apply the convolution smoother

$$S(Z(x, y)) = \int \omega_{(x,y)}(x - x', y - y')Z(x', y')\, d(x', y')$$

where the variance of the kernel $\omega_{(x,y)}$ decreases away from the fault surface. The kernel depends on the fault set and the horizon. This is omitted in the notation in order to simplify. The smoothing makes the horizons close to the faults smoother than the rest of the horizons and it also changes the value of the horizons in well observation. Hence, it is necessary to add a new surface that moves the well observation back to the position before the smoothing and add noise to the smoothed horizons such that these horizons have the same variability everywhere. Then it is necessary that the variability of the noise is the same as the variability that was removed by the smoother. The new horizons are a Gaussian simulation denoted

$$H_{\mathrm{W},2} \sim G(S(F^{-1}(H_{\mathrm{E}})), \sigma_{\omega_{(x,y)}}(x, y), F^{-1}(w))$$

where the three arguments in $G(\cdot, \cdot, \cdot)$ denotes expectation, standard deviation, and data. The final horizons in the second alternative are

$$H_2 = F(H_{\mathrm{W},2}).$$

Slopes

The third alternative is denoted *Slopes*. The faults are represented as slopes in the input horizons denoted H_{S} instead of extrapolating all horizons on both sides of the fault surface. This has been the typical use in a large number of field studies performed by the present Horizon software. The modeled horizons are unfaulted. There may be holes or multiple values in the unfaulted horizons. This is easy to handle in the smoother. This alternative may use exactly the same equations as in the previous alternative but using H_{S} instead of the extrapolated horizons H_{E}. The final realization is defined by the equation

$$H_3 = F(H_{\mathrm{W},3}).$$

Common Properties When Modeling Interpreted Horizons

When modeling interpreted horizons, seismic data in time or depth covering the reservoir may be used. If time data is used, then either the complete modeling may be done in time or it is possible to use the velocity in the trend surfaces or the coefficients in Equation (1). This approach has been used in a large number of field studies, see Abrahamsen (1992).

Reverse faults and faults that are close to vertical with large horizontal uncertainty implies multiple z values in the horizons. A multiple z-value horizon is a horizon with the possibility that there exists two or more points with different z value for the same x and y coordinate. This complicates the modeling and increases the computing (cpu) time and data storage. This may cause problems in all the three alternatives when modeling interpreted horizons. However, when the fault is unfaulted and smoothed, it is easy to fill in wholes and smooth irregularities. Hence, the problem with reverse faults is largest in independent modeling.

For all these three alternatives, it is possible for each horizon set to evaluate the fault set conditioned on the horizon set. This is done by evaluating the smoothness of the unfaulted horizon. A Bayesian approach may be used with the likelihood defined by the equation

$$L_H(F) = \exp\left(-\alpha \int_R (F^{-1}(H(x, y)) - S(F^{-1}(H(x, y))))^2\, d(x, y) \right)$$

for a constant $\alpha > 0$. Note that it is integrated over all the horizons and the entire reservoir R. A posterior distribution for the fault set given the horizons is defined by the product of the prior distribution for the faults and the likelihood defined above. Fault sets may be simulated using a Metropolis–Hastings algorithm. This is very computationally (cpu) intensive if the uncertainty in the faults is large since it will require to simulate a large number of fault sets for each horizon set. An even more computing-time intensive approach is to give a constant prior (noninformative prior) for all horizon sets. This will give a joint posterior distribution for both horizons and faults. These Bayesian approaches may lead to an underestimation of the uncertainty in the faults, if the seismic and horizons are interpreted on the basis of a particular fault model. Then it is better to consider the uncertainty in the horizons and faults as independent except for the adjustment to well data as described in the previous paragraphs.

A less ambitious approach is to generate a limited number of fault sets per horizon set and select one of the faults sets using the likelihood as one of several selection criteria. The likelihood may be calculated in regions around each fault which makes it possible to combine faults from different fault sets in a new fault set. The fault set that was assumed in the seismic processing may be used in the unfaulting and another fault set may be applied in the conditioning and faulting.

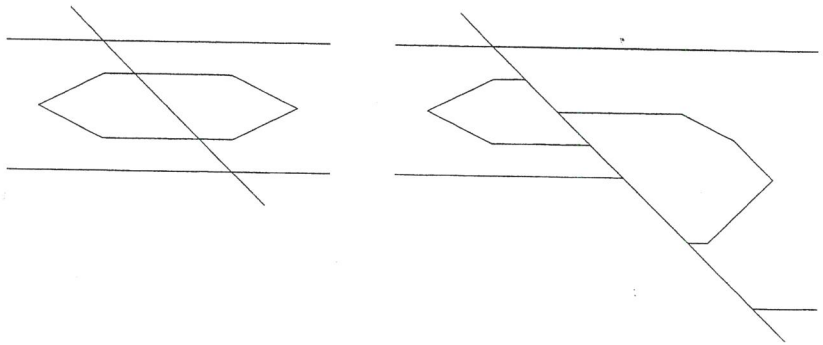

Figure 4. Model of a syn-sedimentary fault where displacement operator is not symmetric on each side of the fault surface. The facies object is much thicker on the right-hand side of the fault.

The use of a displacement operator is best for post-sedimentary faults, but may also be used for syn-sedimentary faults where the displacement operator on one side of the fault surface is not symmetric with the displacement operator on the other side. See Figure 4.

Model Smoothed Horizons

It is also possible to model the smoothed horizons directly as trend surfaces H_T. This approach is most relevant if there is no seismic data since the seismic data describes the horizons after the faulting. The present horizons are obtained by faulting these smoothed input horizons. To satisfy the well data, the fault set F is simulated first and the final horizon set $H_{W,4}$ is found by the simulation

$$H_{W,4} \sim G(H, \sigma, F^{-1}(w)).$$

The final horizons are found by applying the faulting

$$H_4 = F(H_{W,4}).$$

In this alternative, extrapolation of trend surfaces is easier or not needed at all. Reverse faults are handled more easily since the unfaulted input horizons H_T do not need to have multiple z values. The fault operator will transform the smoothed horizons into horizons as they are observed today with multiple z values.

Interaction With Other Parts of the Reservoir Model

The facies and petrophysics are best modeled with the unfaulted horizons as boundaries. This gives continuity from one side of the fault surface to the other.

The fault movement is described in the model, which makes it possible to take into consideration changes in the petrophysics due to the fault. Porosity changes due to compaction are easy to describe. It is more difficult to describe the effect of the fault displacement on other petrophysical variables. Data must be taken through the inverse displacement operator prior to the modeling step.

Building the reservoir simulation grid is an important part of reservoir modeling. It can be done by building a grid as the first step in the workflow and do all the manipulations and calculations on this grid. It can also be done later in the workflow. The grid should then follow the horizons and fault surfaces. Differences in grid topology can have a substantial effect on numerical flow simulation results. To avoid such variations resulting from the different structural realizations, the grid realizations need to have a minimal deviation from one another. The grid building step can sometimes involve a lot of manual editing, which needs to be minimized if multiple realizations are to be generated. One approach for satisfying these partly conflicting criteria is to build a reservoir simulation grid in a usual manner, possibly including much manual work, and then use this grid as a reference grid for other realizations. All the nodes in the reference grid may be defined relatively to the structure i.e. the intersection between a vertical line and a horizon, the intersection between a branch line and a horizontal plane, with equal spacing between other grid nodes, etc. The rest of the grid is defined by equal spacing or some other simple algorithm from the nodes that are defined by the structural model. This approach makes it possible to generate many stochastic generated realizations with a different grid for each realization that follows the structural model. The grids in the different realizations are quite similar and all the manual work is only related to one of these realizations.

AN EXAMPLE

In this section we will present an example illustrating the methodology presented above. Another example from a North Sea case study is reported in a separate paper, see Ottesen and Townsend (in preparation). As mentioned earlier, this structural model has been implemented in the software package Havana (see Hollund and others, 2003). In our applications the faults were represented as slopes in the seismic input horizons. Hence, among the four proposed techniques described in the previous section, we chose to illustrate the *Slopes* method. We will now show how this algorithm can be used to create several different realizations of the faults in a reservoir model.

Figure 5 is a picture of an input horizon to Havana. In the example several horizons are modeled, but only one is shown in the figures. The two largest faults are not included in the stochastic model since the user has sufficient data for these faults and wants to represent these faults deterministically in more detail in other

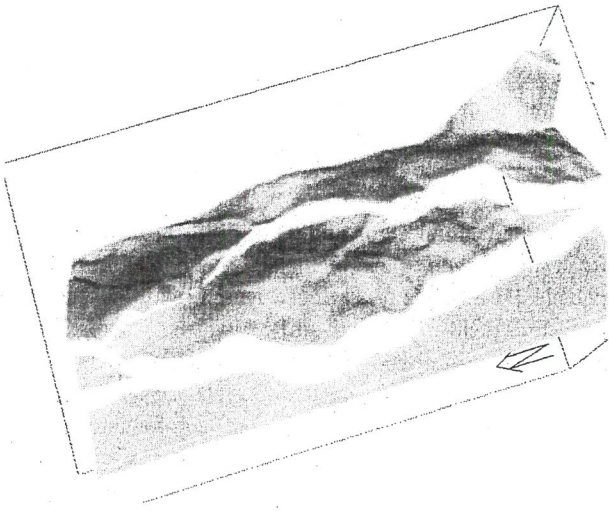

Figure 5. The seismic input horizon to Havana. The surface contains several faults that have been smeared out in the seismic data. Two large faults are not included in the stochastic model and are represented as a discontinuity in the input horizon.

data systems. The horizons contain several steep slopes indicating that large faults are present. In the seismic input data these faults are smeared out.

A geologist has interpreted 18 faults in the reservoir. Figure 6 shows these faults together with the input horizon given in Figure 5.

Figure 7 shows a picture of the horizon produced by the *Slopes* method. More precisely, the *Slopes* algorithm has been applied to the data visualized in Figure 6.

Figure 8 shows a detail in the smooth seismic input and Figure 9 shows a realization of the faults in the same area.

By generating several different realizations, it is possible to quantify the uncertainty. Two uncertainties are particularly useful. The volumes in the different segments may vary quite much between the realizations. If the faults are large and far from vertical, for example in rotated fault blocks, the variation in volume may be large. When drilling new wells close to faults, it is also of major importance to quantify the probability that the new well will intersect the fault. In addition, several realizations may be used in a full field simulation of the reservoir in order to quantify the uncertainty in the reservoir performance.

The model is a full mathematical description that ensures consistency. This example, as indicated by the five pictures described above, shows that it is possible to implement the *Slopes* algorithm and apply the model in a realistic case. The

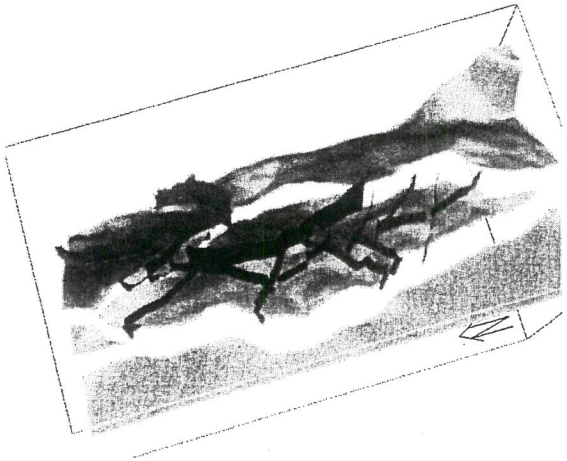

Figure 6. The seismic input horizon together with the 18 faults interpreted by the geologist. Most faults are truncated or truncate other faults.

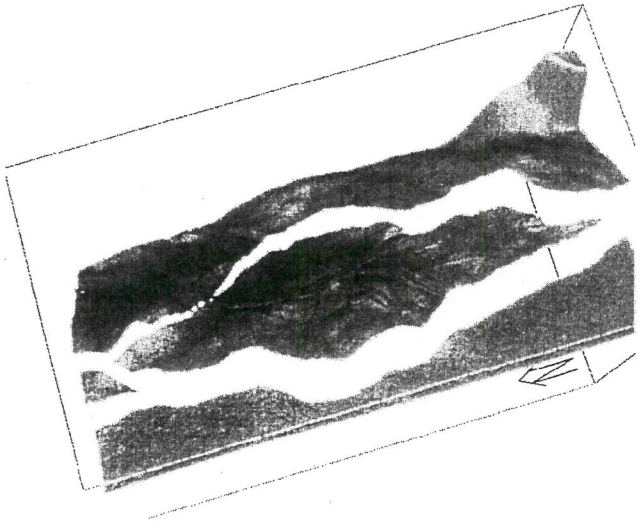

Figure 7. The horizon produced by applying the *Slopes* algorithm in Havana. We see several "sharply" represented faults.

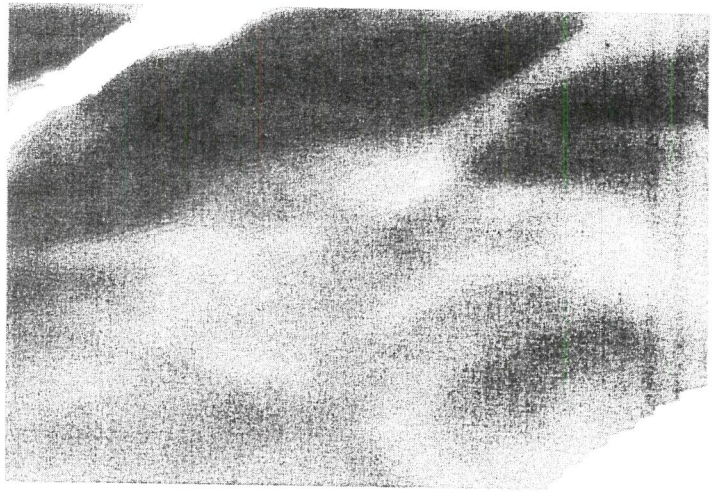

Figure 8. In this picture we have zoomed in on a subregion in the middle of the figure of the horizon shown in Figure 5.

representation of the faults and the horizons were significantly improved using the algorithm and the algorithm-generated faults and horizon that are suitable for the next steps in the modeling procedure. There is no increase in error or artificial slopes in the horizons close to the fault. Integration with the facies and petrophysical model is also easy in this approach.

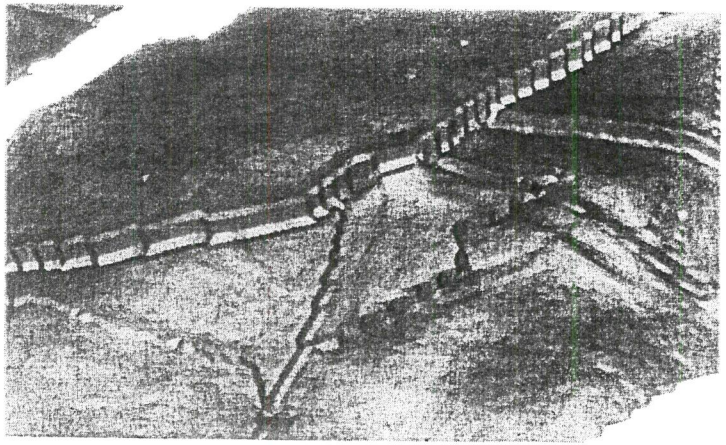

Figure 9. In this picture we have zoomed in on a subregion in the middle of the figure of the horizon shown in Figure 7. The staggered representation of the fault is due to the visualization algorithm.

CONCLUSION

This paper has shown that it is possible to have one consistent stochastic model for both faults and horizons that condition both on well and seismic data. Four different alternatives are described. For all alternatives, it is possible to make many realizations. Quantification of uncertainty may be carried out on the basis of evaluating a set of realizations. The sets may be generated on the basis of a systematic variation of some key parameters, or by only using the stochastic variation.

Independent modeling of faults and horizons is closest to today's practice, but is not able to use information from one side of the fault on the other side and also has problems with controlling the displacement. Both *Independent modeling with displacement* and the *Slopes* alternative avoid these disadvantages at the cost of more operations. *Independent modeling with displacement* requires a time-consuming extrapolation and, in the *Slopes* alternative stronger smoothing is necessary. The final alternative using *Smoothed horizons* is the easiest alternative, but has problems using seismic data.

ACKNOWLEDGMENTS

The authors thank Statoil for funding this research project and allowing the publication of the oil field example. Ariel Almendral Vazquez is thanked for valuable discussions and implementation of part of the algorithms.

REFERENCES

Abrahamsen, P., 1992, Bayesian Kriging for seismic depth conversion of a multi-layer reservoir, *in* Proceedings from Fourth International Geostatistical Congress, Troia, Portugal, September 13–18.

Journel, A. G., and Huijbregts, Ch. J., 1978, Mining geostatistics: Academic Press, New York, 600 p.

Hollund, K., Mostad, P., Nielsen, B. F., and Holden, L., 2000, Havana—A fault modeling tool, *in* Proceedings from the Norw. Petr. Soc. Conference, Stavanger, Norway.

Hollund, K., Mostad, P., Nielsen, B. F., and Holden, L., 2003, Havana web page: www.nr.no

Lia, O., Omre, H., Tjelmeland, H., Holden, L., and Egeland, T., 1997, Uncertainties in reservoir production forecasts: Am. Assoc. Petrol. Geol. Bull., v. 81, no. 5, p. 775–802.

Lindsay, N. G., Murphy, F. C., Walsh, J. J., and Watterson, J., 1993, Outcrop studies of shale smear on fault surfaces, *in* Flint, S. S., and Bryant, I. D., eds., The geological modeling of hydrocarbon reservoirs and outcrop analogues, The International Association of Sedimentologists, Special Publication, No. 15: Blackwell Science, Oxford, p. 113–123.

Manzocchi, T., Walsh, J. J., Nell, P., and Yielding, G., 1999, Fault transmissibility multipliers for flow simulation models: Petrol. Geosci., v. 5, p. 53–63.

Omre, H., and Sølna, K., 1990, Stochastic modeling and simulation of fault zones, *in* Proceedings from The Second CODATA Conference on Geomathematics and Geostatistics, Leeds, England.

Omre, H., Sølna, K., Dahl, N., and Tørudbakken, B., 1992, Impact of fault heterogeneity in fault zones on fluid flow, *in* Aasen, J. O., Berg, E., Buller, A. T., Hjelmeland, O., Holt, R. M., Kleppe, J., and Torsæter, O., eds., Third International Conference on North Sea Oil and Gas Reservoirs, Trondheim, November 30 – December 2, p. 185–200.

Ottesen, S. and Townsend, C., Investigating the effect of varying fault geometry and transmissibility on recovery. Using the (HAVANA-SUM) workflow for structural uncertainty modeling in a clastic reservoir, manuscript in preparation.

Thore, P., Shtuka, A., Lecour, M., Ait-Ettajer, T., and Cognot, R., 2002, Structural uncertainties: Determination, management, and applications: Geophysics, v. 67, no. 3, p. 840–852.

Yielding, G., Freeman, B., and Needham, D. T., 1997, Quantitative fault seal prediction: Am. Assoc. Petrol. Geol. Bull., v. 81, no. 6, p. 897–917.

Mathematical Geology, Vol. 35, No. 8, November 2003 (© 2003)

Spatial Connectivity: From Variograms to Multiple-Point Measures[1]

Sunderrajan Krishnan[2] and A. G. Journel[2]

Anisotropy and curvilinearity are common characteristics of geological structures. Traditional measures of connectivity such as the variogram are rectilinear in that they do not take into account the curvilinearity of these structures. Recent developments in geostatistics have demonstrated and simulated the effect of curvilinearity and multiple-point (mp) connectivity on the output of transfer functions such as flow simulators. A set of curvilinear channels and set of elliptical lenses may share the same variogram and rectilinear connectivity but would yield different flow responses because of their different curvilinearity. A measure of curvilinearity generalizing the variogram measure is therefore proposed. The proposed measure is directional with a tolerance cone and depends on distance with a tolerance, as with an experimental variogram.

KEY WORDS: multiple-point connectivity, curvilinearity.

INTRODUCTION

Geological patterns typically involve simultaneously many locations over possible long distances, they are typically anisotropic and are not rectilinear. Examples are folded surfaces, river channels, and even fault planes that are actually never exactly planar. Modeling of such curvilinear patterns requires measuring the connectivity in the space of the indicators of such structures; the traditional tool offered by geostatistics is the 2-point statistics covariance/variogram which relates any two points in space, for example establishing the probability that any two locations $\mathbf{u}$, $\mathbf{u} + \mathbf{h}$, distant of vector $\mathbf{h}$ be in the same facies. Although already difficult to infer, such variogram statistics is largely insufficient to characterize the shape and spatial continuity of the structure under study, and it should come at no surprise that a model based on only variogram(s) cannot reproduce accurately the structure. Yet continuity of that structure in space may be critical for the application at hand,

[1]Received 23 October 2002; accepted 19 July 2003.

[2]Department of Geology and Environmental Science, Stanford, California 94305; e-mail: sunderk@stanford.edu or journel@pangea.stanford.edu